Journal of Sound and Vibration (2003) **259**(3), 497–512
doi:10.1006/jsvi.2002.5163, available online at http://www.idealibrary.com on IDEAL®

CHAOTIC BEHAVIOR RESULTING IN TRANSIENT AND STEADY STATE INSTABILITIES OF PRESSURE-LOADED SHALLOW SPHERICAL SHELLS

M. S. SOLIMAN

Department of Civil Engineering, Faculty of Engineering, Helwan University, Cairo, Egypt.
E-mail: mssoliman@mail.com

AND

P. B. GONÇALVES

Department of Civil Engineering, Pontifical Catholic University, PUC-Rio, 22435-900 *Rio de Janeiro, Brazil*

(*Received* 18 *April* 2001*, and in final form* 18 *January* 2002)

In this paper, the axisymmetric dynamic behavior and snap-through buckling of thin elastic shallow spherical shells under harmonic excitation is investigated. Based on Marguerre kinematical assumptions, the governing partial differential equations of motion for a pre-loaded cap are presented in the form of a compatibility equation and a transverse motion equation. The continuous model is reduced to a finite degree of freedom system using the Galerkin method and a Fourier–Bessel approach. Results show that pre-loaded shells may exhibit co-existing stable equilibrium states and that with the application of sufficiently large dynamic loads the structure escapes from the well corresponding to pre-buckling configurations to another. This escape load may be much lower than the corresponding quasi-static buckling load. Indeed, complex resonances can occur until the system snaps-through, often signalling the loss of stability. As parameters are slowly varied, steady state instabilities may occur; these can include jumps to resonance, subharmonic period-doubling bifurcations, cascades to chaos, etc. Moreover a sudden pulse of excitation may lead to a transient failure of the system. In this paper, we examine how spherical caps under harmonic loading may be assessed in an engineering context, with a view to design against steady state instabilities as well as the various modes of transient failure. Steady state and transient stability boundaries are presented in which special attention is devoted to the determination of the critical load conditions. From this theoretical analysis, dynamic buckling criteria can be properly established which may constitute a consistent and rational basis for design of these shell structures under harmonic loading.

1. INTRODUCTION

The axisymmetric buckling of shallow spherical shells under quasi-static loading has been extensively studied since the early non-linear investigations by Budiansky [1] and Wienitschke [2]. These were concerned with the large discrepancy between the experimental results and the classical buckling loads. The discrepancies are considered to be due to the high imperfection sensitivity exhibited by these structures. The

0022-460X/02/$35.00

understanding of the non-linear behavior of imperfect shells has contributed to the task of deriving effective design criteria for these shell structures [3]. On the other hand, the dynamic stability analysis of spherical caps has not received the same attention from investigators, possibly because of the difficulties in approaching this problem in a systematic manner, and criteria for dynamic buckling are not well established. Moreover, most of the studies on the axisymmetric dynamic buckling of shallow spherical caps have focused their attention on the snap-through buckling under step loading of infinite or finite duration [4–9]. Relatively little work has been done on the dynamic behavior of spherical caps under harmonic loading [10–14].

Studies have shown that such shells may display, due to their inherently non-linear nature, subharmonic and superharmonic oscillations, period-multiplying bifurcations, multiple solutions, chaotic motions and jumps due to the presence of competing potential wells and non-linear resonance curves within each well. Apart from the works of Gonçalves [12, 15], no work appears to have been consistently done on the more realistic problem of a pre-loaded shell. Simitses [16] has shown that the consideration of static pre-loading is fundamental in the dynamic analysis of structural systems liable to buckling.

In the design of these shells special attention should be given to the phenomenon of *escape* from the potential well associated with the pre-buckling solution. For small forcing amplitudes, the motions remain in the neighborhood of the static non-linear reference state, confined into the pre-buckling well. For certain critical values of the control parameters, the motion may no longer be confined to this well. Here the system may jump into another well or may exhibit large cross-well motions. Such instabilities may cause undesirable stresses or displacements, or ever failure of the structural system. These critical values may be smaller than the corresponding static buckling load and the reduction in the load carrying capacity depends upon the characteristics of the dynamic load. In order to design such a system, one must understand the physical process involved in non-linear dynamic buckling and devise clear criteria and estimates for critical conditions.

Dynamic instability of structural systems liable to buckling can be traced back to the investigations of Budiansky and Hutchinson [17]. Stimulated by recent developments in non-linear dynamics, various investigations have been conducted with the aim of explaining the mechanics of escape from a potential well under various types of dynamic loading and deriving predictive criteria for dynamic buckling. Representative work concerned with basic concepts of dynamic instability and escape from a potential well include references [18–23]. Studies on cylindrical and spherical shells subject to dynamic loads have displayed a wealth of non-linear phenomena [12, 24]. Simplified mass–spring models have also been studied to shed some light on the dynamic behavior and instabilities of limit-point systems [25, 26].

In the present work a non-linear model for the axisymmetric dynamic behavior of clamped shallow spherical shells is presented. The basic approach is to solve the dynamic version of the fourth order Marguerre equations by the Galerkin method. A solution described by a linear combination of Bessel functions and modified Bessel functions based on the free vibration modes of the unloaded perfect cap which is used to determine the non-linear pre-stress state of the cap and to examine its non-linear vibration characteristics along the pre- and post-buckling paths. Each term of the modal expansions satisfies all the relevant boundary and continuity conditions.

The shell under uniformly distributed pressure loading is considered to be initially at rest in a potential well corresponding to a pre-buckling configuration. Then harmonic excitation is applied and conditions for escape from this potential well are sought. The response of the spherical cap is found to be, in many respects, similar to the response of a soft non-linear spring under harmonic load. A comprehensive analysis in parameter space

is conducted and the different ways in which stability is lost are identified. Based on this analysis, clear concepts of dynamic stability or instability are presented including criteria and estimates for critical conditions. Hence, the aim of this study is to provide a better understanding of the dynamic buckling of shallow spherical caps and a basis to construct theoretically well founded and safe lower bound estimates for dynamic buckling loads.

In particular, we examine how such non-linear systems may be assessed, with a view to design against steady state instabilities as well as the various modes of transient failure. By defining steady state and transient stability boundaries, frequency regimes of instability may be identified such that they may be avoided.

Firstly, a steady state analysis is used; resonance response curves in the forcing plane are presented and the main instabilities are identified. *Steady state stability boundaries*, in control space, are then constructed such that the behavior of the system when subjected to a wide range of frequencies and forcing levels may be assessed.

Secondly, the *global transient response* of the system is investigated. The motivation behind such an approach lies in the fact that for typical engineering systems, especially those subjected to just a short duration of excitation, emphasis is on the short-term, rather than the long-term, response of the structure. Since the initial conditions, or even the parameters, may vary widely, and indeed are often unknown, attention is given to analyzing *all* possible transient motions. Hence, the global behavior of the system is examined in terms of transient basins of attraction; safe *basins* can be defined in which transient motions, from a given set of starting conditions, do not exceed a given failure criterion within a specified duration of the excitation [19, 27].

As parameters are varied, such as the forcing frequency for example, basins of attraction can undergo quantitative and qualitative changes; often over a small parameter change there can be rapid erosion and stratification of the basin at a fraction of the forcing level in which the final steady state solution loses its stability; hence a stability analysis which solely considers the steady state and neglects this global transient behavior, may be seriously non-conservative [27–29]. In conclusion, the design implications of this theoretical analysis are assessed; dynamic buckling criteria can be established which may constitute a consistent and rational basis for design of these shell structures under harmonic loading operating under either steady state or transient conditions.

2. BASIC EQUATIONS

The geometry of a uniformly loaded shallow spherical cap with clamped edge conditions is presented in Figure 1, where R, a, H and h are the principal radius of curvature of the sphere, the base radius of the cap, the rise of the mid-surface at the apex and the shell thickness respectively. The polar co-ordinate system in the base plane is defined by r and θ, and the external uniform pressure distributed over the surface of the shell is denoted by q.

Within the framework of shallow shell theory ($H/a < 0{\cdot}25$), the tangential forces and displacements can be taken to be their projections onto the base plane of the shell. The basic equations governing moderately large deformations, but small strains, of shallow spherical caps were formulated by Marguerre [30]. In the case of axisymmetric static deformations of a thin perfect cap, the governing equations may be expressed in the non-dimensional form as

$$\nabla^4 w_s = \lambda^2 \alpha^{1/2} \nabla^2 f_s + Q \frac{4\lambda^4}{\alpha^{1/2}} + \frac{\alpha}{x} \left\{ f_{s,x} \left(w_{s,x} \right) \right\}_{,x}, \tag{1a}$$

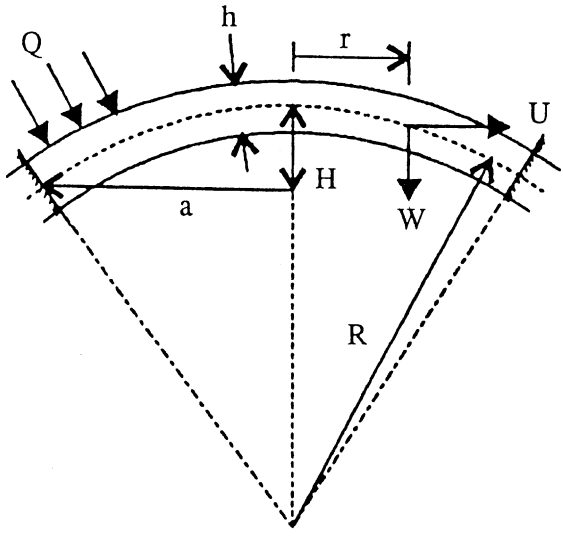

Figure 1. Shell geometry, displacements and co-ordinate system.

$$\nabla^4 f_s = -\lambda^2 \alpha^{-1/2} \nabla^2 w_s - \frac{1}{x}\{w_{s,x} w_{s,xx}\}, \tag{1b}$$

where $(\cdot)_{,x} = \partial/\partial x(\,)$, $\alpha = 12(1-v^2)$ and λ is a geometrical parameter described by

$$\lambda = \alpha^{1/4} a/\sqrt{Rh}. \tag{2}$$

The non-dimensional radial co-ordinate x, the vertical displacement w_s, the stress function f_s, and load parameter Q are related to the corresponding physical quantities by the following relations:

$$x = \frac{r}{a}, \quad w_s = \frac{W_s}{h}, \quad f_s = \frac{F_s}{Eh^3}, \quad Q = \frac{q}{q_{cl}}, \tag{3}$$

where $q_{cl} = 2E(h/R)^2/\sqrt{3(1-v^2)}$ is the classical buckling pressure of a complete spherical shell, E is Young's modulus and v is the Poisson ratio.

The boundary conditions at the clamped edge $x = 1$ of the shallow shell are

$$w_s = 0, \quad w_{s,x} = 0, \quad u_s = f_{s,xx} - \frac{v}{x} f_{s,x} = 0, \tag{4}$$

where u_s is the radial displacement of the shell. Additionally, the finiteness of displacements and stress is required at $x = 0$.

To represent the basic static geometrically non-linear axisymmetric response, the displacement w_s and the stress function f_s are assumed in the form

$$w_s(x) = \sum_{i=1}^{NS} W_{0i}\phi_i(x), \qquad f_s(x) = \sum_{i=1}^{NS} F_{0i}\psi_i(x), \tag{5a, b}$$

where each separate generalized function

$$\phi_i(x) = \mathrm{J}_0(K_i x) + \frac{\mathrm{J}_1(K_i)}{\mathrm{I}_1(K_i)}\mathrm{I}_0(K_i x) - \left[\mathrm{J}_1(K_i)\frac{\mathrm{I}_0(K_i)}{\mathrm{I}_1(K_i)} + \mathrm{J}_0(K_i)\right] \tag{6a}$$

$$\psi_i(x) = \mathrm{J}_0(K_i x) - \frac{\mathrm{J}_1(K_i)}{\mathrm{I}_1(K_i)}\mathrm{I}_0(K_i x) + \frac{K_i^2(\lambda^4 + K_i^4)}{4\lambda^4}\left[\mathrm{J}_1(K_i)\frac{\mathrm{I}_0(K_i)}{\mathrm{I}_1(K_i)} + \mathrm{J}_0(K_i)\right]x^2 \tag{6b}$$

exactly satisfies the clamped boundary conditions at $x=1$ as well as the continuity requirements of displacements and stresses at the center of the shell ($x=0$). These functions are the linear vibration modes of an unloaded clamped shallow spherical shell [11].

In equations (6a) and (6b) J_0 and J_1 are Bessel functions [31], and I_0, and I_1 modified Bessel functions of the first kind, and K_n ($0 < K_1 < K_2 < \cdots$) are the roots of the equation

$$[\mathrm{J}_0(K_n)\mathrm{I}_1(K_n) + \mathrm{I}_0(K_n)\mathrm{J}_1(K_n)]K_n\left[\frac{(\lambda^4 + K_n^4)(1-v)}{\lambda^4 \quad 2} - 1\right] + 2\mathrm{J}_1(K_n)\mathrm{I}_1(K_n)(1+v) = 0. \tag{7}$$

Substituting expressions (5) into equations (1a) and (1b) and applying a Galerkin minimization procedure one obtains a set of $2NS$ non-linear algebraic equations characterizing the static behavior of the cap. Expressions (6a) and (6b) are used as the weighting functions in this Galerkin procedure. These algebraic non-linear equations are solved by the Newton–Raphson method.

In the further analysis, the dynamic behavior of the cap around the axisymmetric non-linear static state will be considered. For this, a dynamic perturbation is superimposed on the basic static state. In this case one has

$$W_p(x,t) = w_s(x) + w(x,t), \qquad F_p(x,t) = f_s(x) + f(x,t), \tag{8a, b}$$

where $w(x,\ t)$ denotes the incremental displacement component and $f(x,t)$ the corresponding incremental stress function.

Using expressions (8) and the dimensionless parameters, one obtains the following non-dimensional equation of motion:

$$\nabla^4 w + w_{,\tau\tau} + \bar{c}w_{,\tau} = \lambda^2\alpha^{1/2}\nabla^2 f + \frac{\alpha}{x}\left\{f_{,x}(w_s + w)_{,x} + f_{s,x}w_{,x}\right\}_{,x} + \frac{4\lambda^4}{\alpha^{1/2}}A_f\ \sin(\Omega\tau) \tag{9a}$$

and the associated compatibility equation

$$\nabla^4 f = -\lambda^2\alpha^{-1/2}\nabla^2 w - \frac{1}{x}\left\{w_{,x}w_{,xx}\right\} + \left[\left(w_{s,x}\right)w_{,x}\right]_{,x}, \tag{9b}$$

where $\gamma^2 = (\alpha a^4\rho/eh^2)$ and

$$\tau = t/\gamma, \quad \bar{c} = \gamma c/\rho h, \quad \Omega = \gamma\omega. \tag{10}$$

Here ρ is the mass density, t is the time, ω is the driving frequency and c is the damping coefficient.

The incremental state is assumed in the separable form

$$w(x,\tau) = \sum_{i=1}^{ND} W_i(\tau)\phi_i(x), \qquad f(x,\tau) = \sum_{i=1}^{ND} F_i(\tau)\psi_i(x). \tag{11a, b}$$

The substitution of expressions (11) into equations (9a) and (9b), the use of the complete equations for the basic non-linear static state, and the application of the Galerkin method

yield a set of $2ND$ non-linear equations characterizing the dynamic behavior of the pre-loaded cap.

The interested reader may find a more detailed presentation of the formulation used in this paper as well as a parametric analysis of the static and dynamic behavior of the cap under pressure loading in reference [3], where the non-linear buckling behavior of an imperfect cap was analyzed, and in reference [12, 15] where the free vibration characteristics and the non-linear response of the cap under harmonic loading was studied.

3. ONE-DEGREE-OF-FREEDOM MODEL

In a dissipative system, energy is lost due to damping and the system may settle down to a final motion which can be described by only a few dimensions. This allows one to use various mathematical techniques and numerical tools recently developed for the global investigation of low-dimensional systems. In particular, one can examine the global behavior of the system in terms of transient basins of attraction or safe basins in which transient motions, from a given set of starting conditions, do not exceed a given failure criterion within a specified duration of the excitation [19, 27, 32]. It will be assumed for this study, based on numerical results, that for shallow spherical caps the first mode is dominant and a simplified one-degree-of-freedom (1 d.o.f) model is capable of describing with a reasonable degree of accuracy the non-linear behavior of the cap; issues such as modal coupling which might result in internal resonances will be considered in future research. Nonetheless, results considering several degrees of freedom for both the static and dynamic response have obtained the same general behavior and bifurcation scenario as the one presented in this paper [12].

Using in expressions (5) the number of terms NS necessary to achieve convergence of the non-linear static state and using only one mode ($ND = 1$) in equation (11) to describe the dynamic response, one obtains a 1-d.o.f. model for the cap. Elimination of F_1 in the resulting equation of motion by the use of the compatibility equation results in the following equation of motion in terms of W_1:

$$W_{1,\tau\tau} + \bar{c}W_{1,\tau} + \alpha_1 W_1 + \alpha_2 W_1^2 + \alpha_3 W_1^3 = \beta A_f \sin(\Omega\tau), \tag{12}$$

where the coefficients α_i and β are functions of the shell parameters and of the static pre-stress state.

As one can observe, equation (12), governing the motion of the pressure loaded cap, possesses both quadratic and cubic non-linearities. Elimination of both damping and forcing will produce the equation

$$W_{1,\varsigma\varsigma} + \alpha_1 W_1 + \alpha_2 W_1^2 + \alpha_3 W_1^3 = 0. \tag{13}$$

Multiplying equation (13) by $W_{1,\tau}$ and integrating will yield

$$\tfrac{1}{2} W_{1,\tau}^2 + \tfrac{1}{2}\alpha_1 W_1^2 + \tfrac{1}{3}\alpha_2 W_1^3 + \tfrac{1}{4}\alpha_3 W_1^4 = C, \tag{14}$$

where $T = 1/2 W_{1,\tau}^2$ is recognized as the kinetic energy, $\Pi = \alpha_1 W_1^2/2 + \alpha_2 W_1^3/3 + \alpha_3 W_1^4/4$ is seen to be the potential energy and C is a constant.

Table 1 shows the values of the coefficients α_i for a cap with $\lambda = 4$ and $v = 1/3$ under selected static load levels.

The static non-linear response for this shell is shown in Figure 2. For $Q < Q_L$, only one equilibrium point (a point attractor) exists. For $Q_L < Q < Q_U$ there are three equilibrium points: two stable equilibrium positions separated by a saddle. In this range one has a non-symmetric two-well potential function. Increasing the load in this range, the well, associated with the buckled state, becomes deeper, while the well, associated with the

TABLE 1

Load Q	α_1	α_2	α_3
0·00	612·77	−581·51	154·24
0·10	552·16	−559·53	154·24
0·20	486·40	−534·34	154·24
0·30	413·34	−504·41	154·24
0·40	328·67	−466·48	154·24
0·50	219·87	−410·50	154·24

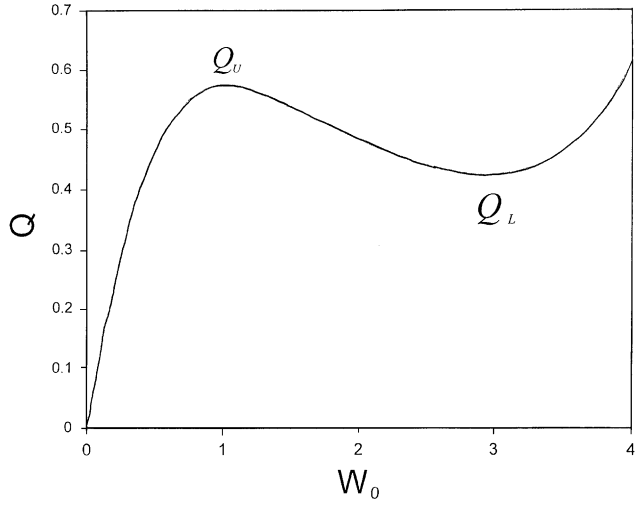

Figure 2. Non-linear equilibrium path of a shallow shell, $\lambda = 4$.

unbuckled state, becomes shallower. The existence of these competing attractors for $Q_L < Q < Q_U$ is the main source of the complex non-linear dynamic behavior shown herein.

For a perfect cap with $\lambda = 4$ and $v = 1/3$ and $Q = 0{\cdot}5$, equation (12) reduces to

$$W_{1,\tau\tau} + \bar{c}W_{1,\tau} + 219{\cdot}87W_1 - 410{\cdot}50W_1^2 + 154{\cdot}24W_1^3 = 358{\cdot}88A_f \sin(\Omega\tau). \qquad (15)$$

For this load level there are three equilibrium positions at $W_1 = 0$, 0·7431 and 1·9183. These are in fact the values of the temporal amplitudes of the first mode. To obtain the spatial equilibrium configurations, these values should be inserted into equation (11a) and multiplied by the corresponding spatial interpolating function. For instance, the corresponding displacement of the apex of the shell are 0, 1·1518 and 2·9734. The shape of the corresponding potential is illustrated in Figure 3, showing two smooth minima at $W_1 = 0$ and 1·9183, where the damped, unforced system has point attractors and a maximum at $W_1 = 0{\cdot}7431$, corresponding to a saddle point. A small external vibration converts these static equilibrium points to limit cycles in the forced system. For the rest of this study, we shall use numerical time integrations, using a fourth order Runge–Kutta algorithm, to analyze the large amplitude motions of equation (15), since analytical methods become increasingly inaccurate at higher amplitudes which often result in chaotic vibrations.

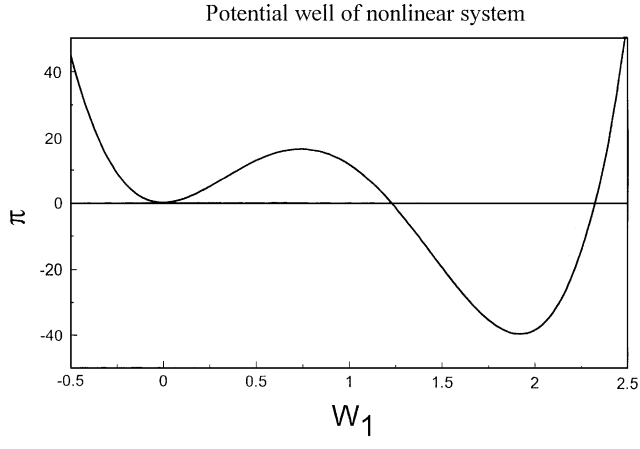

Figure 3. Potential well of the non-linear system.

Firstly, the *steady state response*, namely that in which transients have effectively decayed, will be determined. Secondly, attention will be turned to the *global transient behavior* of the system. By acknowledging that the system from the initial conditions $(W_1(0), \dot{W}_1(0))$ can experience various combinations of excitations, one can say that the four-dimensional phase-control space $((W_1(0), \dot{W}_1(0), A_f, \Omega))$ defines the ensuing motion. To determine a safe transient basin, each integration is continued until the system either exceeds a given failure criterion, or the maximum number of forcing cycles, m, is reached, implying that the system is safe or robust to such an excitation. In this way one can define a set of points in the four-dimensional space that do not fail within m cycles and hence define a transient safe basin. Since only the transient behavior is being assessed, no note is made of the type of attractor the system settles upon. There may be indeed many co-existing attractors, which may include the harmonic, subharmonic or even chaotic attractors.

Specifying the controls and taking a grid in the $(W_1(0), \dot{W}_1(0))$ plane allows us to draw conventional cross-sections in the phase-space of the initial conditions: while specifying $(W_1(0), \dot{W}_1(0))$ and taking a grid in the (A_f, Ω) plane allows one to draw cross-sections of transient basins in the two-dimensional control space.

4. STEADY STATE STABILITY BOUNDARIES

4.1. STEADY STATE RESONANCE

For systems operating under essentially steady state conditions, where transients have effectively decayed, the variation of a parameter can result in a resonance response, where at critical frequencies, the system may execute large amplitude oscillations or indeed completely lose its stability and fail. In this section typical non-linear resonance behavior is outlined, and the main or fundamental instabilities identified. Response curves under the slow variation of forcing amplitude are shown in Figure 4 where the maximum steady state displacement (during one facing period) has been plotted against the forcing amplitude, A_f, at fixed Ω.

As the forcing is applied, the systems leaves the stable equilibrium state, starts to oscillate in a transient manner and then settles down to a steady state $n=1$ oscillation of period $T=2\pi/\Omega$. The transient length and the amplitude of oscillation are dependant upon

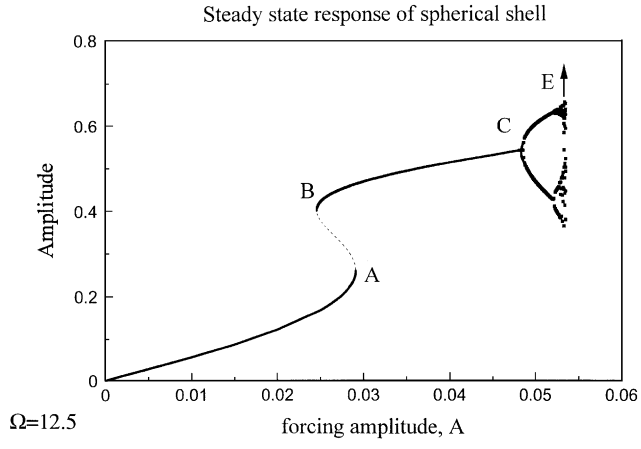

Figure 4. Steady state response curve at $\Omega_N = 12{\cdot}5$, $c = 2{\cdot}0$.

the damping level of the system. For small amplitude oscillations, the system behaves like a linear oscillator, as can be seen in the almost linear relationship between W_{max} and A_f. However, at higher forcing levels, non-linear behavior is evident, where it can be seen that a small increase in A_f results in a relatively large change in W_{max}. Indeed a region of hysteresis is observed between A and B. A further increase in A_f results in a more gradual increase in amplitude until then $n = 1$ oscillation becomes inversely unstable and there is a period-doubling flip bifurcation, at C, to an $n = 2$ subharmonic oscillation of period $T = 4\pi/\Omega$. The period-doubling scenario is again repeated at diminishing scales with an infinite cascade of flip bifurcations running through subharmonics of order $2,4,8,\ldots,\infty$ which generates a chaotic attractor. The stable attracting solution of the steady state chaos finally loses its stability at a boundary crisis, at E, which results in the inevitable escape out of the potential well (left hand) with the amplitude tending to large values. In the engineering sense this would imply failure of the system.

In this summary, it has been shown that under the slow variation of a parameter qualitative changes in the behavior of the system can occur. Such bifurcations may be considered as dangerous instabilities since they may often result in a substantial quantitative change in the response. At points A and B for example, the system experiences jumps to and from resonance, respectively; at C the harmonic response loses its stability and becomes a subharmonic responses; at E, the chaotic oscillation loses its stability at a crisis.

4.2. STEADY STATE BOUNDARIES IN PARAMETER SPACE

In this section steady state stability boundaries, that identify regimes of the various modes of instability are constructed. Figure 5 shows the main steady state bifurcations, in (A_f, Ω) control space, in the frequency regime close to the fundamental resonance (the natural frequency $\Omega_N = 14{\cdot}82$)

Line A represents parameters in which jumps to resonance occur. Line B corresponds to a saddle-node fold, which results in the creation of a finite amplitude oscillation (a jump from B may occur). Line C is the first period-doubling flip bifurcation, at which this resonant harmonic attractor period-doubles to a stable subharmonic of order $n = 2$. There is an infinite sequence of these flip bifurcations leading to a chaotic attractor which finally

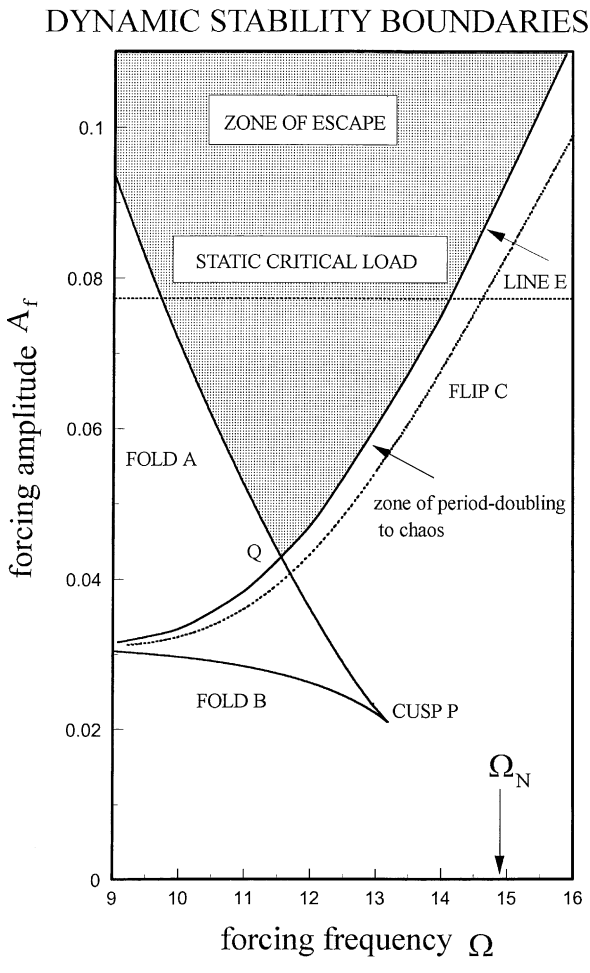

Figure 5. Steady state stability boundaries in (A_f, Ω) parameter space.

loses its stability at a crisis at E. Point Q corresponds to where line E intersects line A. For jumps to resonance occurring from fold A above point Q, there are no available attractors to jump to within the right-hand well, and hence a purely deterministic but unsafe jump occurs where the system fails. Also shown is the value of the static critical load.

5. GLOBAL TRANSIENT DYNAMICS: EROSION OF THE SAFE BASIN

Since several steady state attractors may co-exist at a fixed set of control parameters the initial conditions, $(W_1(0), \dot{W}_1(0))$ play an important role in the eventual long-term response of the system (see Figure 6). For many engineering system, however, especially those subjected to just a short-duration excitation, emphasis is on the short-term, rather than the long-term, response of the structure. Since the initial conditions may vary widely, and indeed are often unknown, it is useful to address the transient global behavior of the system in terms of transient basins of attraction. Studies have shown that it may be convenient to describe the evolution of the safe basin as the magnitude of the excitation is increased [19].

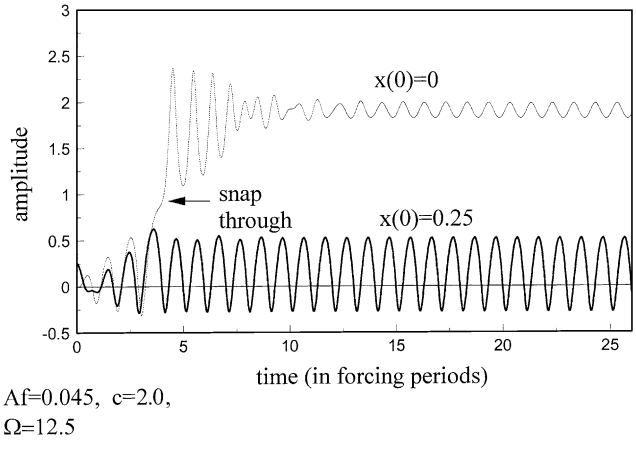

Figure 6. Sensitivity of the response to the initial conditions. Two different initial conditions may lead to a (i) safe response, (ii) snap through at $A_f = 0{\cdot}045$, $\Omega = 12{\cdot}5$.

Figure 7 shows a basin evolution sequence as the excitation is increased. Here, from a grid of initial conditions, each integration is continued until either the response exceeds a given failure criterion, W_{max}, or the maximum allowable number of cycles, $m(=20)$, is reached and hence the system is considered to be *safe* or robust to such an excitation. The choice of both the failure criterion (say a given displacement or velocity, for example) and m depends on the system in question.

Since only the transient behavior of the system is being assessed, no note is made to which attractor the system settles. There may be indeed many co-existing attractors, which may include the harmonic, subharmonic or even chaotic attractors. Here, white represents the safe, or the non-escaping, basin and black represents the unsafe basin. It can be seen that there is little change in the size or position of the safe basin up to $A_f = 0{\cdot}035$. As the magnitude of the forcing is increased there is then a homoclinic tangling of the stable and unstable manifolds of the hill-top saddle, resulting in a fractal basin boundary, with thin finger-like projections penetrating the safe basin. This results in a sensitive dependence on the initial conditions; however, on the macroscopic level, this phenomenon is not too serious provided that this fractal zone remains as a thin layer around the edge of the basin. As the forcing is further increased, these fingers become more evident until at $A_f = 0.045$, due to underlying manifold organization and consequent heteroclinic events, there is a dramatic erosion and stratification of the basin.

This rapid loss of basin area can be quantified by engineering integrity curves. Figure 8 shows how the basin area, G, determined by recording the proportion of initial starts that do not fail with m forcing cycles within the given window of initial conditions, varies with the magnitude of excitation [19]. In comparison with Figure 4, it can be clearly seen that the loss of basin area occurs at smaller forcing level, than that at which the steady state attractor loses it stability at a crisis, E. Due to the inherent uncertainties in the specification of the initial conditions, this represents a rapid loss of integrity for a system operating in an ill-defined environment. Although there remains a residual basin, associated with the steady state attractor, an engineering analysis, which considers *only* a steady state stability analysis, and neglects this global transient behavior, might therefore be seriously non-conservative.

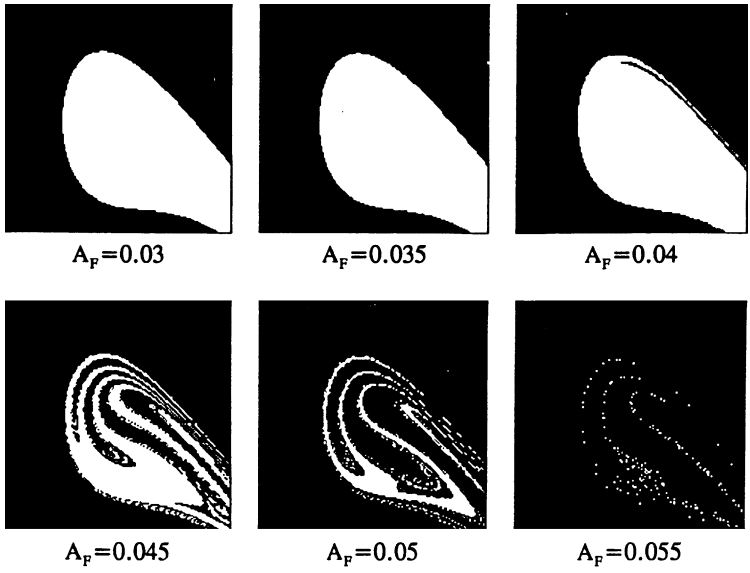

Figure 7. Global transient behavior may be assessed plotting basins of attraction versus forcing amplitude A_f. Here $\Omega_N = 12{\cdot}5$. For each picture 150×150 initial conditions are chosen in the window $-0{\cdot}8 < W(0) < 1, -10 < \dot{W}(0) < 10$. Maximum number of forcing cycles ($m = 20$) or a failure criterion (W_{max}) = 1 is reached. White indicates safe basin; black indicates unsafe basin.

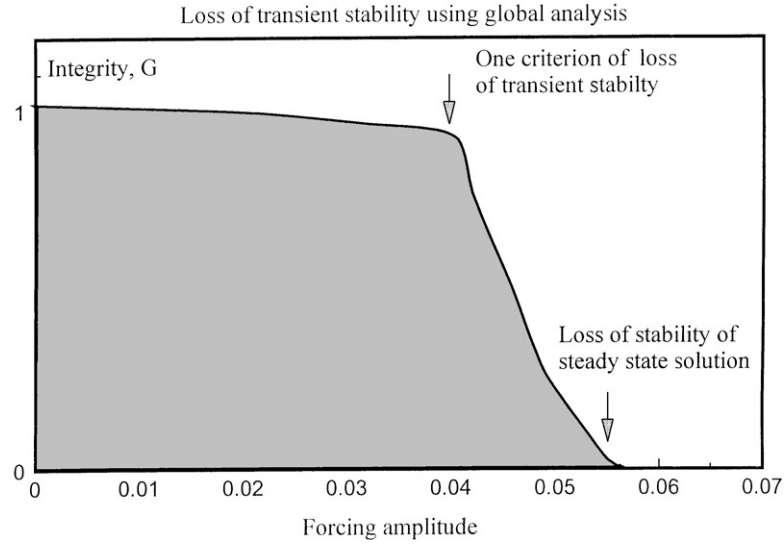

Figure 8. Global integrity curve, of safe basin area versus A_f. Here $\Omega_N = 12{\cdot}5$ shown. Here G is the normalized safe basin area (safe basin area at Af/safe basin area $A_f = 0$) and 50×50 initial conditions are chosen in the window $-0{\cdot}8 < W(0) < 1, -10 < \dot{W}(0) < 10$. Maximum number of forcing cycles ($m = 20$) and the failure criterion is $W_{max} = 1$.

6. FRACTAL BOUNDARIES IN PARAMETER SPACE

In this section transient boundaries in *parameter-space* are assessed by considering the response of the system from a fixed set of initial conditions to a wide combination of excitation parameters. The fractal control boundaries in parameter space would in some

sense correspond to the classical pictures of Mandelbrot. The set of (A_f, Ω) values that can sustain such a pulse indefinitely is here a set of *absolute constraint*, corresponding to the Mandelbrot set; whereas the control values that prevent escape with m forcing cycles would define a set of *transient constraint*.

A typical transient time map in control space for fixed initial conditions is shown in Figure 9. Here starting all time integrations from an initial condition at the equilibrium $(W_1(0), \dot{W}_1(0) = 0)$ and using a grid in control space gives us the (A_f,Ω) cross-sections of the safe basins. The reason here for choosing initial conditions close to the equilibrium state, would for example, allow the failure locus of a this structural system resting near its ambient equilibrium state to a sudden pulse of excitation of magnitude A_f and frequency Ω, to be determined. Furthermore, since the phase-basin is often swiftly eroded across its entire region, the global loss of engineering integrity may be detected by time integrations

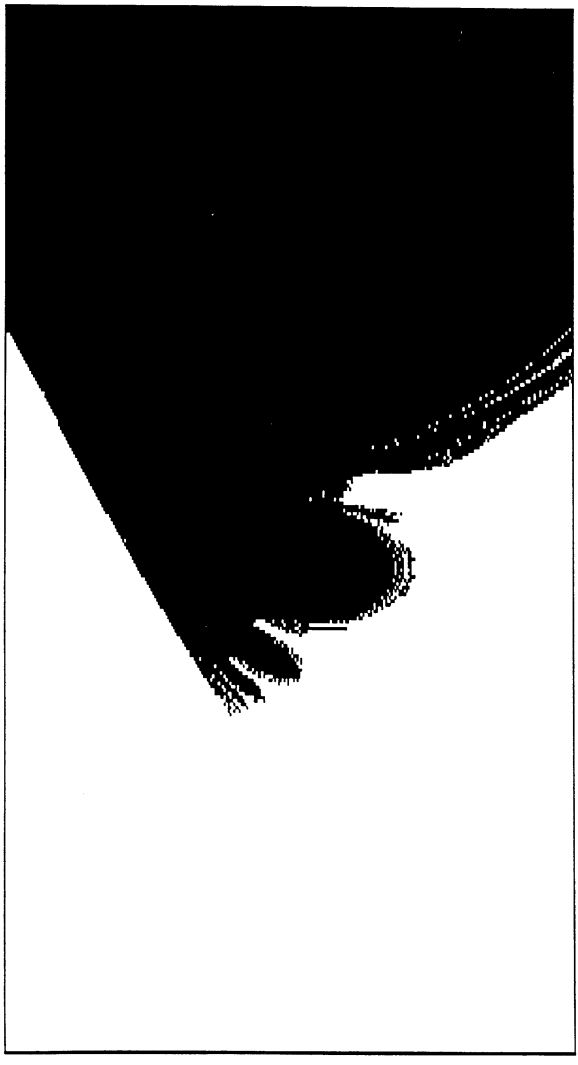

Figure 9. Transient time map in (A_f,Ω) parameter space. For this diagram the range of (A_f,Ω) correspond to Figure 5 and $W(0) = \dot{W}(0) = 0$. Maximum number of forcing cycles ($m = 20$) and a failure criterion is chosen at $W_{max} = 1$. White indicates safe basin; black indicates unsafe basin.

from a small number of starting conditions at a given set of parameters. For many practical purposes (especially in terms of computational effort, or indeed model testing) an adequate assessment may be obtained by just one central start. Here, it must be recalled that the four-dimensional *phase-control space* $(W_1(0), \dot{W}_1(0)_1, A_f, \Omega)$ defines the ensuing motion. Since one is interested in analyzing the global transient response in terms of the phase-basin structure, choosing other initial conditions near the equilibrium, would result in the same macroscopic structure of these control-space transient-time maps. Obviously in the fractal regimes, the response would be infinitely sensitive to the choice of initial states.

Regions that are unsafe (escape), with W tending to large values, within m forcing cycles are shaded in black; regions that remain safe (bounded) are shaded in white. This diagram clearly summarizes the excitations the system can sustain. In comparison with the stability boundaries for steady state one sees that for relatively small forcing levels, the initial condition chosen generates a response that remains with the well. However at higher forcing levels, one can see that the boundaries in control-space become *fractal* such that there is now a sensitive dependence on parameters. There is a highly interwined zone in which some parameters generate trajectories that remain bounded and some result in escape out of the well; an increase of the forcing level at a fixed frequency does not necessarily imply escape out of the well. On the practical level these fractal boundaries, in which the response is infinitely sensitive to the parameters, may be considered as a failure locus for a system subjected, while resting near its ambient state, to a sudden pulse of excitation, since both short- and long-term predictability is lost.

On the macroscopic level, this analysis also provides information regarding the characteristics of the initial condition map, and hence the global transient stability of the system. Since the phase-space basin is often swiftly eroded across its entire region, by choosing an initial condition near the central zone, the global loss of engineering integrity may for practical purposes be adequately assessed from such an analysis.

7. CONCLUSIONS

Based on Marguerre's shallow shell equations, an accurate multi-mode solution is formulated and applied to study the non-linear vibration characteristics of a pressure-loaded geometrically perfect spherical cap along its non-linear pre- and post-buckling paths. It is shown that pressure-loaded shallow spherical shells exhibit a high degree of non-linearity.

A detailed parametric study, using computer simulations, shows that the cap under harmonic excitation may display dynamic buckling loads well below the static limit-load. In particular it has been shown that for systems which operate under essentially steady state conditions, large amplitude, subharmonic and chaotic oscillations may occur as well as dangerous bifurcations that may result in failure of the system. On the other hand, for systems operating in essentially transient conditions, where the global basin behavior is of importance, large-scale erosion and stratification of the basin implies a loss of transient stability of the system. It was examined how steady state and transient stability boundaries, that identify regimes of instability, may be constructed, such that non-linear structural systems under vibration may be designed accordingly.

The global transient stability of a typical thin-walled structure has been assessed and quantified in terms of transient basins of attraction. It was shown that under increasing excitation, basin boundaries can become fractal; although this fractal zone may initially be confined to a small region of phase-space, a relatively small parameter change may result in rapid erosion and stratification of the whole basin. It was argued that this represented a

loss of global transient stability of the system. In addition, it was shown that a stability analysis based solely on the steady state response may be seriously non-conservative.

Furthermore, it was shown that boundaries in parameter space can become fractal. Since in all dynamical systems there is uncertainty in the specification of the parameter values, these diagrams clearly summarize the excitations the system can sustain. By choosing initial conditions near the equilibrium solution, the failure locus of a system resting near its ambient equilibrium state due to a sudden pulse of excitation of magnitude A_f and frequency Ω may be determined. Furthermore, since the phase-space basin is often swiftly eroded across its entire region, the global loss of engineering integrity may, from a practical point of view, be assessed using this approach.

It is suggested that the present study can provide a basis for design criteria for shallow spherical shells under harmonic loads. Although the analysis of shells under harmonic loading provides an understanding of the resonant behavior, it may also provide a basis for analyzing the response to other types of periodic loads, and in some aspects, under other types of time varying load. This may have importance, for example, when analyzing the failure of shell structures under wind loading [33]; and in the dynamic analysis of shallow spherical shells, in the context of biomedical engineering, where they have been used in ventricular assist devices [34, 35]. Here, a shallow elastic spherical cap separates the blood chamber from the pneumatic chamber and is subjected to a periodic loading; where the snap-through phenomenon is responsible for the desired blood flow. In the analysis of such devices, the correct type of periodic response and the reliability of such response under pressure fluctuations is essential to patient survival.

Although the present analysis is restricted to clamped spherical caps, some of the conclusions could be extended to other thin-walled structural elements liable to fold-type buckling such as shallow conical caps, cylindrical panels and shallow arches. In addition other issues which may have an important influence on the dynamic instability of the shell include the type of loading, modal coupling, with the possibility of internal resonances, the influence of geometric imperfections as well as non-symmetric effects will all be considered topics of future research.

REFERENCES

1. B. Budiansky 1959 *Proceedings of the IUTAM Symposium on the Theory of Thin Elastic Shells. Delft, The Netherlands*, 64–94. Buckling of clamped shallow spherical shells.
2. H. J. Weinitschke 1960 *Journal of Mathematics and Physics* **38**, 209–231. On the stability problem for shallow spherical shells.
3. P. B. Gonçalves and J. G. A. Croll 1992 *American Society of Civil Engineers Journal of Structural Engineering* **118**, 970–985. Axisymmetric buckling of pressure-loaded spherical caps.
4. B. Budiansky and R. S. Roth 1962 *Collected Papers on Instability of Shell Structures, NASA TN D*-1510, 597–606. Axisymmetric dynamic buckling of clamped shallow spherical shells.
5. N. C. Huang 1969 *American Institute of Aeronautics and Astronautics Journal* **7**, 215–220. Axisymmetric dynamic snap-through of elastic clamped shallow spherical shells.
6. G. J. Simitses 1974 *Journal of Applied Mechanics* **41**, 299–300. On the dynamic buckling of shallow spherical caps.
7. R. Kao and N. Perrone 1978 *Computers and Structures* **9**, 463–473. Dynamic buckling of axisymmetric spherical caps with initial imperfections.
8. P. C. Dumir, M. I. Gandhi and Y. Nath 1984 *ACTA Mechanica* **52**, 93–106. Axisymmetric static and dynamic buckling of orthotropic shallow spherical caps with flexible supports.
9. W. J. Shao and P. A. Frieze 1989 *Thin-Walled Structures* **8**, 99–118; 183–201. Static and dynamic numerical analysis studies of hemispheres and spherical caps. Part I: Background and theory. Part II: Results and strength predictions.

10. H. A. Evensin, and R. M. Evan-Iwanowski 1967 *American Institute of Aeronautics and Astronautics Journal* **5**, 969–976. Dynamic response and stability of shallow spherical shells subjected to time-dependent loading.
11. K. Yasuda, and G. Kushida 1984 *Bulletin of JSME* **27**, 2233–2240. Nonlinear forced oscillations of a shallow spherical shell.
12. P. B. Gonçalves 1996 In *Proceedings of the 2nd European Nonlinear Oscillations Conference*. (L. Prust and F. Peterka, editors), Vol. 3, 91–94. Prague, Czech Republic: Publishing House of Czech Technical University. Axisymmetric non-linear dynamic response and instabilities of shallow spherical shells.
13. Z. M. Ye, 1997 *Journal of Sound and Vibration* **202**, 303–311. The non-linear vibration and dynamic instability of thin shallow shells.
14. P. L. Grossman, B. Koplit and Y. Yu 1969 *American Society of Mechanical Engineers* **36**, 451–458. Nonlinear vibrations of shallow spherical shells.
15. P. B. Goncalves 1994 *Journal of Sound and Vibration* **174**, 249–260. Axisymmetric vibrations of imperfect shallow spherical caps under pressure loading.
16. G. J. Simitses 1983 *American Institute of Aeronautics and Astronautics Journal* **21**, 1174–1180. Effects of static preloading on the dynamic stability of structures.
17. B. Budiansky and J. W. Hutchinson 1964 *Proceedings of the 11th International Congress of Applied Mechanics, Munich, Germany*. Dynamic buckling of imperfection-sensitive structures.
18. J. M. T. Thompson 1989 *Proceedings of Royal Society of London* **A421**, 195. Chaotic phenomena triggering the escape from a potential well.
19. M. S. Soliman and J. M. T. Thompson 1989 *Journal of Sound and Vibration* **135**, 453–475. Integrity measures quantifying the erosion of smooth and fractal basins of attraction.
20. D. Dinkler and B. Kröplin 1991 In *Buckling of Shell Structures on Land, in the Sea and in the Air* (J. F. Jullien, editor), pp. 83–91. London: Elsevier. An energy based concept for dynamic stability of elastic structures.
21. L. N. Virgin, R. H. Plaut and C. Cheng 1992 *International Journal Non-Linear Mechanics* **27**, 357–365. Prediction of escape from a potential well under harmonic excitation.
22. M. S. Soliman 1993 *Journal of Applied Mechanics* **60**, 669–676. Jumps to resonance: long chaotic transients, unpredictable outcome, and the probability of restabilization.
23. W. Szemplinska-Stupnicka 1995 *Nonlinear Dynamics* **72**, 129–147. The analytical predictive criteria for chaos and escape in nonlinear oscillators: a survey.
24. A. H. Nayfeh and R. A. Raouf 1987 *American Society of Mechanical Engineers Design Analysis Plates Shells* **105**, 145. Nonlinear forced response of circular cylindrical shells.
25. N. A. Kounadis and J. Raftoyiannis 1990 *American Institute of Aeronautics and Astronautics Journal* **28**, 1217–1223. Dynamic stability criteria of nonlinear elastic damped/undamped systems under step loading.
26. N. A. Kounadis and D. S. Sophianopoulos 1996 In *Structural Dynamics — EURODYN'96* (A. Augusti, C. Borri and P. Spinelli, editors) 671–679. Rotterdam, The Netherlands: Balkema. Nonlinear dynamic buckling of a cylindrical shell panel model.
27. J. M. T. Thompson and M. S. Soliman 1990 *Proceedings of the Royal Society of London* **A428**, 1–13. Fractal control boundaries of driven oscillators and their relevance to safe engineering design.
28. M. S. Soliman 1994 *ASME Proceedings of Engineering Systems Design and Analysis: Structural Dynamics and Vibration, London, U.K.* (B. Ovunc et al, editors) Vol. 7, 345–350. Design of non-linear systems under vibration: boundaries of steady state instabilities and chaotic transient failure.
29. M. S. Soliman 1994 *Nonlinear Dynamics* **6**, 317–329. Global transient dynamics of parametrically excited systems.
30. K. Marguerre 1939 *Jahrbuch der* 1939 *der deutschen Luftfahrtforschung*, 413. Zur Theorie der gekrümmten platte grosser Formänderung.
31. M. Abramovitz and I. A. Stegun 1964 *Handbook of Mathematical Functions.* New York, NY: Dover Publications.
32. M. S. Soliman 1995 *Journal of Sound and Vibration* **182**, 729–740. Fractal erosion of basins of attraction in coupled nonlinear systems.
33. M. Levy and M. Salvadori [1992] *Why Buildings Fall Down.* New York, W. W. Norton and Co.
34. J. R. Rowles, B. L. Mortimer and D. B. Olsen 1993 *ASAIO Journal* **39**, 840–855. Ventricular assist and total artificial heart devices for clinical use.
35. Y. Senzai 2001 *Artificial Organs* **25**, 318–322. Progress and future perspectives in mechanical circulatory support.